Structural, Magnetic, and Transport Properties of $(La_{1+x}Sr_{1-x})CoRuO_6$ Double Perovskites

Jan-Willem G. Bos and J. Paul Attfield*

Department of Chemistry, University of Cambridge, Lensfield Road, Cambridge, CB2 1EW, United Kingdom, and School of Chemistry and Centre for Science at Extreme Conditions, University of Edinburgh, West Mains Road, Edinburgh, EH9 3JJ, United Kingdom

Received February 13, 2004. Revised Manuscript Received March 5, 2004

The structures, magnetism, and electronic transport properties of $(La_{1+x}Sr_{1-x})CoRuO_6$ ($-0.50 \le x \le 0.25$) double perovskites have been investigated. All samples are found to crystallize with the monoclinic $P2_1/n$ superstructure. An increase of antisite disorder with $|x|$ is found to be controlled by a reduction in the average charge and size difference between the Co and Ru states. Neutron diffraction results for $(LaSr)CoRuO_6$ show the presence of a long-range, ordered antiferromagnetic state with propagation vector ($^1/_2$ 0 $^1/_2$) below 85 K. Hole doping ($x < 0$) enhances the Neel temperature slightly, whereas electron doping ($x > 0$) results in a sharp decrease. Resistivity measurements showed all compositions to be variable-range-hopping semiconductors, where hole doping decreases the resistivity by 2 orders of magnitude, but electron doping has a much less pronounced effect.

Introduction

A large number of double perovskites with B-cation ordering of transition-metal cations have been prepared since the 1950s (ref 1). Some of these perovskites, including Sr_2FeMoO_6 and Sr_2FeReO_6, are found to be itinerant ferrimagnets that display large low-field magnetoresistances.[2,3] The itinerancy and ferrimagnetism arise from a double exchange type mechanism in which ordering and electronic configurations of the transition-metal cations play a critical role.[4] Structurally, the 3d (B) and 4d or 5d (B′) transition metal cations are ordered in an alternating (rocksalt) manner within a perovskite lattice. Electronically, the 3d cation has a large spin ($S = 2$ to $^5/_2$ for Fe^{2+}−Fe^{3+}) whereas the 4d or 5d cation usually has $S \le {}^1/_2$. We are studying new analogous materials in which both of the B site cations have substantial magnetic moments, such as Co^{2+} and Ru^{5+}, which both have $S = {}^3/_2$. Here we present a study of the $(La_{1+x}Sr_{1-x})CoRuO_6$ system, which displays control of electronic properties both by doping and by cation inversion (Co/Ru antisite disorder), as well as an unusual, indeterminate magnetic structure. The $x = 0$ phase was previously reported (ref 5) to be a 3D variable-range-hopping (VRH) semiconductor that orders magnetically at $T = 157$ K. Recently, we have presented a study into the analogous $(La_{1+x}Ca_{1-x})CoRuO_6$ system.[6]

Experimental Section

Initial studies showed that homogeneous $(La_{1+x}Sr_{1-x})CoRuO_6$ solid solutions could be prepared for $-0.50 \le x \le 0.25$ by solid-state reaction. Stoichiometric amounts of La_2O_3 (99.9+%), $SrCO_3$ (99.9+%), Co_3O_4 (99.9+%), and RuO_2 (99.9%) were ground, pressed into pellets, and heated for a total of 48 h at 1200 °C (with three intermediate regrinding steps). All samples were deemed to be phase pure, as X-ray powder diffraction (XPD) patterns collected on a Philips PW1710 diffractometer showed no impurity reflections to be present.

Magnetic susceptibilities were measured using both an Oxford Instruments vibrating sample magnetometer (VSM) and a Quantum Design SQUID. The temperature (50−300 K) dependence of the electrical resistivity was measured using a Quantum Design Physical Property Measurement System and a Keithley K236 source measurement unit. All samples were measured in zero magnetic field and in $H = 1000$ Oe.

The crystal and magnetic structures of $(LaSr)CoRuO_6$ have been investigated using neutron powder diffraction (NPD). NPD experiments were performed on the high-resolution D2B diffractometer at the Institute Laue Langevin in Grenoble, France. Data were collected in the $5 \le 2\theta \le 160°$ range in 0.05° increments at 4 K, and between 30 and 300 K in 30 K intervals. The neutron wavelength was 1.5946 Å. The GSAS suite of programs was used for Rietveld fitting of the NPD and XPD data.[7,8] A pseudo-Voigt function convoluted with an axial divergence contribution was used to describe the peak shape for both XPD and NPD data.

Results and Discussion

X-ray Diffraction. Rietveld analysis of the XPD data showed all $(La_{1+x}Sr_{1-x})CoRuO_6$ ($-0.50 \le x \le 0.25$) compounds to crystallize with the monoclinic $P2_1/n$ superstructure commonly found in double perovskites.[1] Figure 1 illustrates the ordered double perovskite

* To whom correspondence should be addressed. E-mail: j.p.attfield@ed.ac.uk.

(1) Anderson, M. T.; Greenwood, K. B.; Taylor, G. A.; Poeppelmeier, K. R. *Prog. Solid State Chem.* **1993**, *22*, 197−233.
(2) Kobayashi, K. L.; Kimura, T.; Sawada, H.; Terakura, K.; Tokura, Y. *Nature* **1998**, *395*, 677−680.
(3) Gopalakrishnan, J.; Chattopadhyay, A.; Ogale, S. B.; Venkatesan, T.; Greene, R. L.; Millis, A. J.; Ramesha, K.; Hannoyer, B.; Marest, G. *Phys. Rev. B* **2000**, *62*, 9538−9542.
(4) Sarma, D. D. *Curr. Opin. Solid State Mater. Sci.* **2001**, *5*, 261−268.
(5) Kim, S. H.; Battle, P. D. *J. Solid State Chem.* **1995**, *114*, 174−183.
(6) Bos, J. W. G.; Attfield, J. P. *Phys. Rev. B* In press.
(7) Larson, A. C.; von Dreele, B. B. General Structural Analysis System (GSAS), report LAUR 86-748, Los Alamos National Laboratory, 1994.
(8) Rietveld, H. M. *J. Appl. Crystallogr.* **1969**, *2*, 65−71.

10.1021/cm0497733 CCC: $27.50
Published on Web 04/08/2004

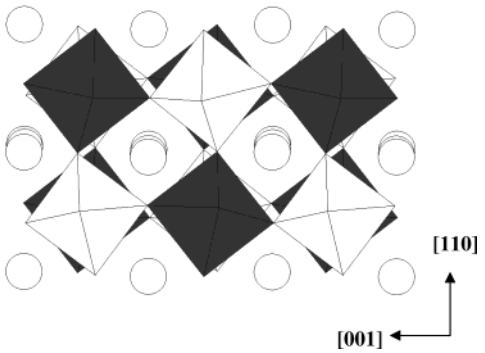

Figure 1. View of the structure of monoclinic (LaSr)CoRuO$_6$ at 300 K. Shaded/unshaded polyhedra are occupied by Co/Ru.

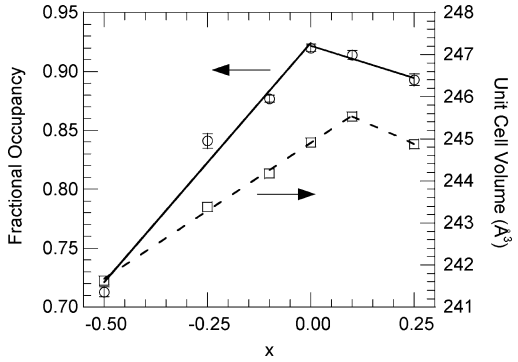

Figure 2. Fractional occupancy of the majority B and B′ cations (circles) and unit cell volumes (squares) for (La$_{1+x}$Sr$_{1-x}$)-CoRuO$_6$.

structure for the $x = 0$ compound at 300 K, as determined from NPD data. The cell volume is found to increase linearly from $x = -0.50$ to 0.10, indicating the formation of a solid solution (Figure 2), although an anomalous contraction is observed for $x = 0.25$. The $P2_1/n$ superstructure allows for a rocksalt ordered arrangement of Co and Ru over the perovskite B-sites, whereas La and Sr are randomly distributed over the A-sites. Rietveld analysis shows a small degree of Co/Ru disorder (8% inversion) for $x = 0$ and a larger degree of disorder for both $x < 0$ and $x > 0$ (Figure 2).

As reported for the M = Ca analogue (ref 6), two potential causes of Co/Ru antisite disorder in (La$_{1+x}$M$_{1-x}$)CoRuO$_6$ (M = Ca,Sr) can be distinguished. One cause is a reduction in size and charge difference between the average Co and Ru states. Anderson et al. have shown that B-cation charge and size differences are critical for obtaining a high degree of rocksalt ordering in double perovskites, and a formal charge difference of ≥3 between transition-metal cations is usually required.[1] Assuming the presence of only Co^{2+} and Ru^{5+} states at $x = 0$ (which is confirmed by bond valence sum calculations, Table 2 and ref 6), then doping with M ($x < 0$) or La ($x > 0$) results in the partial oxidation of Co^{2+} or reduction of Ru^{5+}, respectively. The presence of Co^{3+} ($x < 0$) or Ru^{4+} ($x > 0$) reduces the average charge and size differences between Co and Ru sites compared to $x = 0$, and therefore antisite disorder increases with $|x|$.

The second possible cause of Co/Ru antisite disorder is the random strain field resulting from the A-site La/M disorder. The presence of quasirandomly arranged A-cations results in structural disorder on the A-sites that can be quantified using the statistical size variance[9] $\sigma^2 = \langle r_A^2 \rangle - \langle r_A \rangle^2$. The A-cation size variance is an important parameter in controlling the physical properties of perovskite materials, such as the Curie temperature of the CMR manganites and the superconducting transition of the high-T_c cuprates.[9] Any coupling between A-site and B-site disorder will be maximal for $x = 0$, where the A-site variance is largest, $\sigma^2 = 3.24 \times 10^{-4}$ Å^2, (M = Ca) or $\sigma^2 = 22.09 \times 10^{-4}$ (M = Sr), and decreases with increasing $|x|$. The B-site disorder is found to be minimal for $x = 0$ in both series of (La$_{1+x}$M$_{1-x}$)CoRuO$_6$ compounds (8% inversion for M = Sr and no inversion for M = Ca) and increases with $|x|$ (ref 6 and Figure 2). Therefore, the increase in antisite disorder for $x < 0$ and $x > 0$ can be attributed to a decreasing average charge and size difference of the Co and Ru states. The difference in B-site ordering observed for the $x = 0$ compositions is in keeping with the relatively large amount of A-site disorder present for M = Sr.

Magnetic Properties. The temperature dependence of the field-cooled (FC) ($H = 100$ Oe) magnetic susceptibilities of the (La$_{1+x}$Sr$_{1-x}$)CoRuO$_6$ compounds are shown in Figure 3a. A ferromagnetic ordering transition at ~170 K is observed for all samples and the onset does not change significantly with x. The absence of a magnetic ordering transition at ~170 K in the neutron diffraction patterns of the $x = 0$ phase, combined with the identical ordering temperatures for all x, suggests that the ferromagnetism is due to a small amount of SrRuO$_3$, which is known to order magnetically at 140−167 K (refs 10,11). Furthermore, no ferromagnetism was observed in the (La$_{1+x}$Ca$_{1-x}$)CoRuO$_6$ analogues, and the possible analogous CaRuO$_3$ impurity phase is antiferromagnetic (ref 6). Figure 3b shows the temperature dependence of the zero-field-cooled (ZFC) susceptibility for the $x = 0$ composition, measured in $H = 100$ Oe. The ZFC susceptibility has a maximum at 85 K that is associated with the Neel transition to long-range antiferromagnetic ordering in the principal LaSrCoRuO$_6$ phase, as discussed later. The additional shoulder at ~150 K is due to the ferromagnetic SrRuO$_3$ contribution. Under ZFC conditions, the limited alignment of magnetic domains in this magnetically soft material leads to a smaller magnetization than under FC conditions (Figure 3a), enabling the paramagnetic to antiferromagnetic transition in the principal phase to be seen. The Neel temperatures of the other compositions could also be determined from the ZFC susceptibilities and are given in Table 1. For $x < 0$, T_N increases slowly to a maximum of 91 K ($x = -0.50$), whereas for $x > 0$, T_N decreases rapidly to 52 K ($x = 0.25$), signaling a strong asymmetry for hole ($x < 0$) and electron ($x > 0$) doping. The field dependence of the magnetization (Figure 3c) for $x = 0$ at 20 K features a small hysteresis on an essentially linear (antiferromagnetic) background. Extrapolation of the linear regions indicated a saturation magnetization $M_{sat} \approx 0.1$ emu/g, which corresponds to a 1.5% SrRuO$_3$ impurity (taking $M_{sat} = 15$ emu/g for SrRuO$_3$, ref 10). Comparison of the FC susceptibilities at 50 K (Figure 3a) indicates a SrRuO$_3$ impurity of ~2%

(9) Attfield, J. P. *Chem. Mater.* **1998**, *10*, 3239−3248.
(10) Joy, P. A.; Date, S. K.; Kumar, P. S. A. *Phys. Rev. B* **1997**, *56*, 2324−2327.
(11) Reich, S.; Tsabba, Y.; Cao, G. *J. Magn. Magn. Mater.* **1999**, *202*, 119−122.

Table 1. Fitted Unit Cell Data, Neel Temperatures, and Curie−Weiss Parameters for the $(La_{1+x}Sr_{1-x})CoRuO_6$ Double Perovskites

x	−0.50	−0.25	−0.10	0	0.1	0.25
a (Å)	5.5764(2)	5.5863(2)	5.5877(2)	5.5903(2)	5.5894(2)	5.5887(2)
b (Å)	5.5374(2)	5.5484(2)	5.5561(2)	5.5639(2)	5.5731(2)	5.5645(2)
c (Å)	7.8250(2)	7.8522(2)	7.8648(2)	7.8744(2)	7.8822(2)	7.8740(2)
β (deg)	90.05(1)	90.01(1)	90.03(1)	90.03(1)	90.04(1)	90.05(1)
T_N (K)	91	90	88	85	70	52
μ_{eff} (μ_B/fu)	5.43	6.31	6.41	5.37	5.78	6.19
θ (K)	8	−40	−43	−15	−40	−31

for the $x < 0$ samples and of ~0.5% for $x > 0$, in agreement with the changing La/Sr ratio.

Paramagnetic moments and Weiss temperatures (Table 1) were determined from Curie−Weiss fits to the susceptibility data in the $180 < T < 300$ K range. All Weiss temperatures (Table 1) are negative with small magnitudes, indicating the presence of antiferromagnetic interactions, except for $x = -0.50$, which has $\theta = 8$ K. The effective moment found for $x = 0$ ($\mu_{eff} = 5.4$ μ_B/fu) is close to the expected spin-only value ($\mu_{eff} = 5.5$ μ_B/fu) assuming the presence of Co^{2+} (high spin) and Ru^{5+} states. The gradual increase in μ_{eff} observed for electron doping ($x > 0$, Table 1) was also observed for the analogous $(La_{1+x}Ca_{1-x})CoRuO_6$ compounds and is inconsistent with a local spin approximation where reduction of $4d^3$ (t_{2g}^3) Ru^{5+} to low-spin $4d^4$ (t_{2g}^4) Ru^{4+} decreases the predicted spin-only moment to 5.3 μ_B/fu for $x = 0.25$. For hole doping ($x < 0$), no trend is observed (Table 1), contrary to the gradual increase in μ_{eff} found for $(La_{1+x}Ca_{1-x})CoRuO_6$.

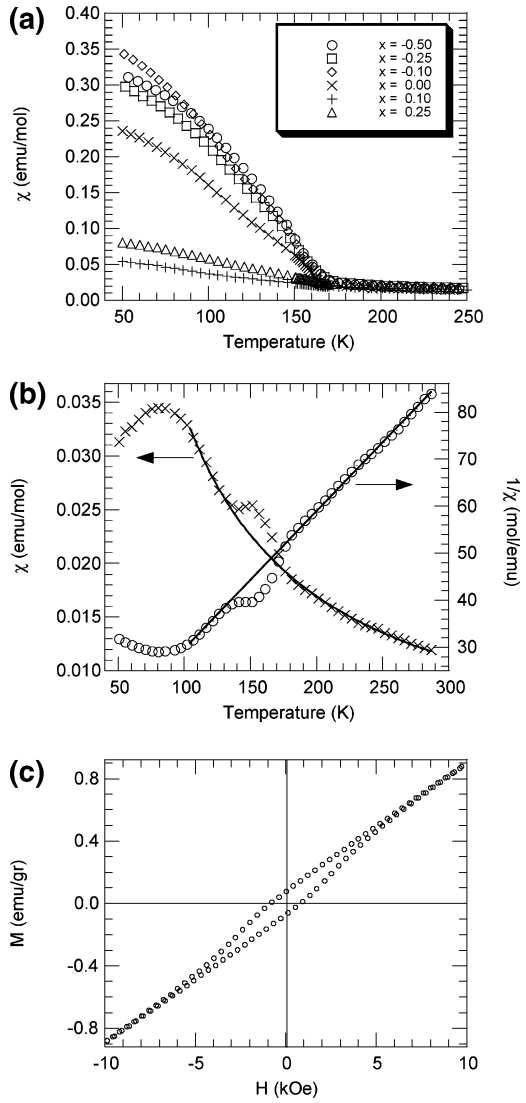

Figure 3. (a) Field-cooled ($H = 100$ Oe) magnetic susceptibilities for $(La_{1+x}Sr_{1-x})CoRuO_6$, (b) zero-field-cooled magnetic susceptibility and inverse susceptibility for $(LaSr)CoRuO_6$ (the solid lines correspond to Curie−Weiss fits), and (c) magnetization-field hysteresis loop for $(LaSr)CoRuO_6$.

Transport Properties. All $(La_{1+x}Sr_{1-x})CoRuO_6$ compositions were found to be VRH semiconductors. The temperature dependence of the resistivity was fitted in the $50 < K < 300$ K range (Figure 4a,b) using a VRH equation with Mott prefactor[12]

$$\rho(T) = \rho_0\sqrt{T/T_0}\,\exp^{(T_0/T)^{1/(d+1)}}$$

where d is the dimensionality of the variable-range-hopping process ($d = 3$). The onset of magnetic ordering does not result in any resistivity anomalies. The fitted T_0 parameter has a maximum value (2.8×10^8 K) for $x = 0$ and decreases for $x > 0$ and $x < 0$, indicating a lower energy barrier for the hopping process (Figure 5). The resistivities decrease by almost 2 orders of magnitude for hole doping ($x < 0$) but change much less significantly for electron doping ($x > 0$) (Figure 5). Excess Sr

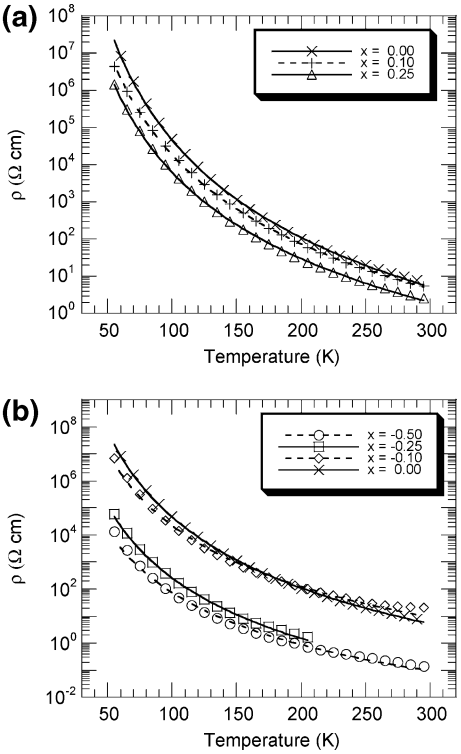

Figure 4. Temperature dependence of the resistivities for $(La_{1+x}Sr_{1-x})CoRuO_6$, (a) with $x \geq 0$ and (b) $x \leq 0$. The lines correspond to fits using the VRH model.

Table 2. Refined Atomic Parameters for (LaSr)CoRuO$_6$ at 300 K (Top Entries) and 4 K (Bottom Entries) and 300 K Fractional Occupancies and Bond Valence Sums (BVS) for the Metals Indicated and Oxygen Sites[a]

atom	position	*x*	*y*	*z*	*B* (Å^2)	occupancy	BVS
La/Sr	4e	0.0033(6)	0.0218(4)	0.251(1)	0.60(4)	0.50/0.50	La: 2.72(2)
		0.0042(5)	0.0259(3)	0.251(1)	0.14(3)		Sr: 2.35(2)
Co/Ru1	2c	0.5	0	0.5	0.14(4)	0.94(1)/0.06(1)	Co: 2.40(2)
					−0.08(4)		
Co/Ru2	2d	0.5	0	0	0.14(4)	0.06(1)/0.94(1)	Ru: 4.83(3)
					−0.08(4)		
O1	4e	0.2886(8)	0.280(1)	0.0355(6)	0.48(13)	1.00	2.03(2)
		0.2933(7)	0.279(1)	0.0351(6)	0.16(12)		
O2	4e	0.2324(9)	0.774(1)	0.0264(7)	0.98(13)	1.00	1.98(2)
		0.2309(8)	0.777(1)	0.0280(6)	0.48(11)		
O3	4e	−0.0662(5)	0.4938(6)	0.255(1)	0.64(7)	1.00	2.07(2)
		−0.0684(4)	0.4937(5)	0.252(1)	0.22(5)		

[a] Residuals for the 300 K fit: $\chi^2 = 1.60$, $R_{WP} = 5.48\%$, $R_P = 4.30\%$, $R_F^2 = 3.95\%$. Residuals for the 4 K fit: $\chi^2 = 2.69$, $R_{WP} = 4.96\%$, $R_P = 3.90\%$, $R_F^2 = 3.57\%$.

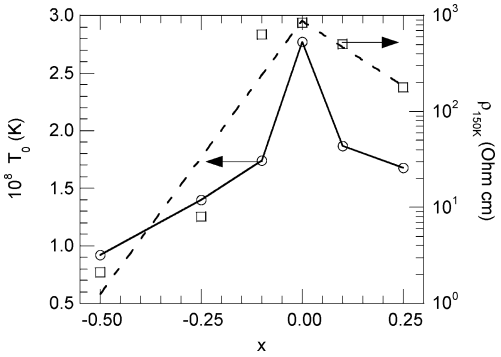

Figure 5. The fitted T_0 VRH parameter and resistivities at 150 K for (La$_{1+x}$Sr$_{1-x}$)CoRuO$_6$.

($x < 0$) is expected to introduce holes (Co^{3+} states) in the Co^{2+} t_{2g} band, and the conductivity measurements show that these have an enhanced mobility over the intrinsic charge carriers. Electron doping ($x > 0$) evidently creates local Ru^{4+} states in the Ru^{5+} t_{2g} band that do not have a significantly higher mobility. None of the samples showed a significant magnetoresistance effect between zero field and $H = 1000$ Oe.

Neutron Diffraction, Crystal Structure. The temperature dependencies (4−300 K) of the structural parameters of (LaSr)CoRuO$_6$ were determined by Rietveld fitting of the D2B NPD data. The nuclear patterns at 4 and 300 K are almost identical, with no evidence for any structural transition in this temperature range. No diffraction peaks for $SrRuO_3$ were observed. The atomic coordinates, occupancies, isotropic temperature factors, and selected bond lengths and bond angles at 300 and 4 K are given in Tables 2 and 3. Neutron diffraction showed a 6% inversion of Co and Ru, which is comparable to that observed by X-ray diffraction (8% inversion). Bond valence sums[13] (BVS) are given in Table 2 and are consistent with the presence of Co^{2+} and Ru^{5+} states. It must be noted that the bond valence sums using the observed metal−oxygen bond lengths provide the only accurate experimental information on the Co/Ru oxidation states. The paramagnetic moment of 5.4 μ_B/fu does not distinguish between the theoretical spin-only moments of Co^{2+} + Ru^{5+} ($\mu_{eff} = 5.5$ μ_B/fu) and high-spin Co^{3+} + Ru^{4+} ($\mu_{eff} =$ 5.7 μ_B/fu). Furthermore, the absence of a unique solution to the magnetic structure (see below) prevents the saturation moments of Co and Ru from being unambiguously determined.

Table 3. Selected Bond Distances (Å) and Bond Angles (deg) for (LaSr)CoRuO$_6$ at 300 and 4 K[a]

	300 K	4 K
La/Sr−O1	2.735(9)	2.730(8)
La/Sr−O1	2.448(9)	2.447(9)
La/Sr−O1	2.771(10)	2.748(9)
La/Sr−O1	3.252(8)	3.269(8)
La/Sr−O2	2.581(8)	2.563(8)
La/Sr−O2	2.688(9)	2.677(8)
La/Sr−O2	2.792(10)	2.778(9)
La/Sr−O2	3.114(9)	3.148(8)
La/Sr−O3	2.962(4)	2.986(3)
La/Sr−O3	2.654(4)	2.637(3)
La/Sr−O3	2.449(4)	2.437(3)
La/Sr−O3	3.150(4)	3.152(3)
Co−O1	2.043(5)	2.063(4)
Co−O2	2.012(6)	2.020(5)
Co−O3	2.038(8)	2.019(8)
⟨Co−O⟩	2.031(4)	2.034(3)
Ru−O1	1.976(6)	1.954(5)
Ru−O2	1.966(6)	1.958(5)
Ru−O3	1.969(9)	1.985(8)
⟨Ru−O⟩	1.970(4)	1.966(4)
Co−O1−Ru	157.6(3)	157.1(3)
Co−O2−Ru	164.8(3)	163.5(3)
Co−O3−Ru	158.6(2)	157.9(1)

[a] Co and Ru labels refer to sites Co/Ru1 and Co/Ru2 in Table 2, respectively.

The contraction of the unit cell volume upon cooling (Figure 6a) is adequately described by the following equation

$$V(T) = V_0 + A \coth\left(\frac{T_D}{T}\right)$$

where $T_D = 116(8)$ K is the Debye temperature, $V_0 = 243.1(1)$ Å^3 is the unit cell volume at $T \rightarrow 0$, and $A = 0.63(6)$ is a fitting constant. The *a*-axis also shows a gradual contraction with temperature (Figure 6b), whereas the contractions of the *b*- and *c*-axis are less gradual (Figure 6a,b).

The temperature dependencies of the octahedral Co−O and Ru−O bond lengths are given in parts a and b of Figure 7, respectively. The average Co−O and Ru−O bond lengths do not decrease significantly in the 4−300 K range (Table 3). The average Co−O−Ru bond angle is found to decrease gradually on going from 300

(12) Mott, N. F. *Metal Insulator Transitions*; Taylor and Francis: London, 1974.

(13) Bond Valences were calculated using the Valist program (Wills, A. S.; Brown, I. D.; CEA: France, 1999) using standard parameters except for $R_0 = 1.89$ Å for Ru(V)−O, which is taken from ref 6.

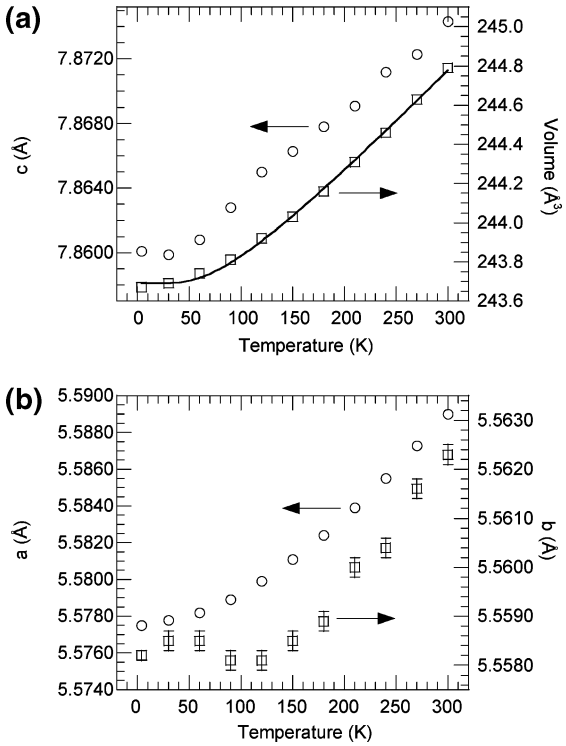

Figure 6. Temperature dependence of (a) the *c*-axis and unit cell volume and (b) the *a*- and *b*-axis in (LaSr)$CoRuO_6$.

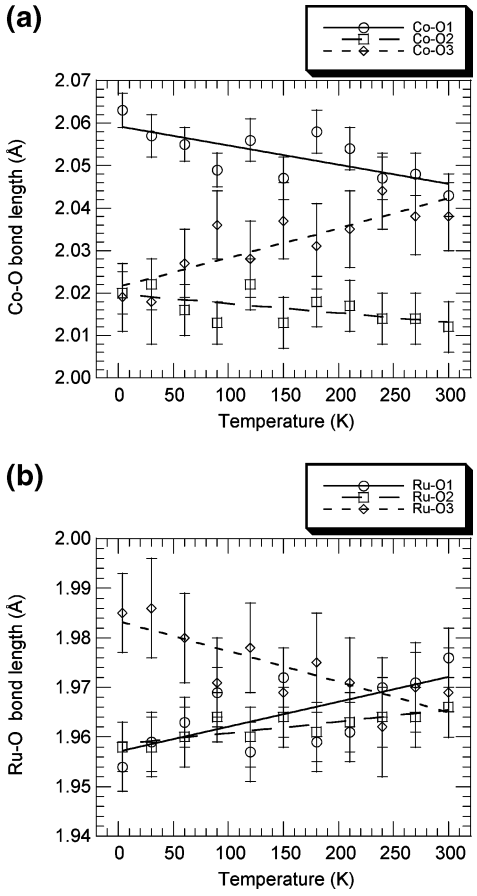

Figure 7. Thermal evolution of (a) Co−O and (b) Ru−O bond lengths in (LaSr)$CoRuO_6$ with linear fits.

to 90 K and then remains constant down to 4 K (Figure 8). At 300 K the RuO_6 octahedra are undistorted, whereas the CoO_6 octahedra have two short and four

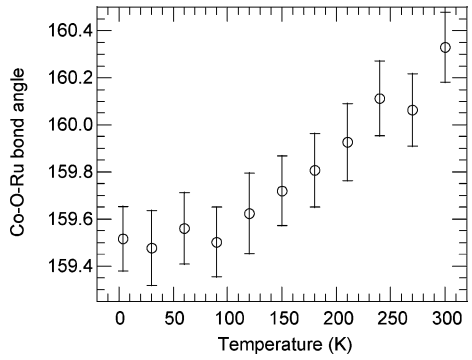

Figure 8. Thermal evolution of the average Co−O−Ru bond angle (deg) in (LaSr)$CoRuO_6$.

long bonds. Upon cooling both the CoO_6 and RuO_6 octahedra gradually distort to give four short and two long bonds at 4 K. The Co^{2+} high-spin $3d^7$ electronic configuration has a ^4T ground state in octahedral symmetry and so is susceptible to a Jahn−Teller distortion that can result in a tetragonal elongation with two long and four short bonds. This corresponds to the situation at 4 K but is exactly opposite to the CoO_6 octahedral distortion at 300 K. No discontinuities in the cell constants have been observed that could signal the occurrence of a magnetostrictive anomaly at T_N, as for example observed in (LaCa)$CoRuO_6$ (ref 6) and in CoO (ref 14). Therefore, the small distortions of the BO_6 octahedra in the 300−4 K range probably result from the thermal contraction of the structure rather than a Jahn−Teller distortion or a magnetostrictive anomaly associated with the onset of long-range magnetic ordering at 85 K. The significant antisite disorder for (LaSr)-$CoRuO_6$ (6−8% inversion) compared to (LaCa)$CoRuO_6$ (no inversion) may suppress a possible magnetostriction at the Neel transition.

Neutron Diffraction, Magnetic Structure. Magnetic reflections were observed below 90 K (Figure 9) and no evidence for any long-range magnetic ordering transition was found at 170 K. The magnetic reflections were all indexed by a propagation vector of ($^1/_2$ 0 $^1/_2$), showing that antiferromagnetic Co and Ru sublattices are present. A symmetry representation analysis of the possible spin arrangements has previously been reported[15] for the analogous monoclinic double perovskite Sr_2MnMoO_6, which also has the ($^1/_2$ 0 $^1/_2$) magnetic propagation vector but only one magnetic B cation sublattice (Mn). That study showed that four Mn spin representations gave equally good fits to the powder neutron diffraction data, in part because the monoclinic cell distortion is too small to resolve (*hkl*) and ($hk\bar{l}$) magnetic reflections.

Determination of the magnetic structure of (LaSr)-$CoRuO_6$ is complex, because two magnetic B cation sublattices (Co and Ru) are present. All of the four spin representations in ref 15 were found to give equally good fits to the powder neutron data. Furthermore, for any model, the magnitudes of the Co and Ru moments are very highly correlated, so that refinements with spin only at Co, only at Ru, or some intermediate combination gave equivalently good fits. Refinement of the spin

(14) Greenwald, S. *Acta Crystallogr.* **1952**, *6*, 396.
(15) Munoz, A.; Alonso, J. A.; Casais, M. T.; Martinez-Lope, M. J.; Fernandez-Diaz, M. T. *J. Phys.: Condens. Matter* **2002**, *14*, 8817−8830.

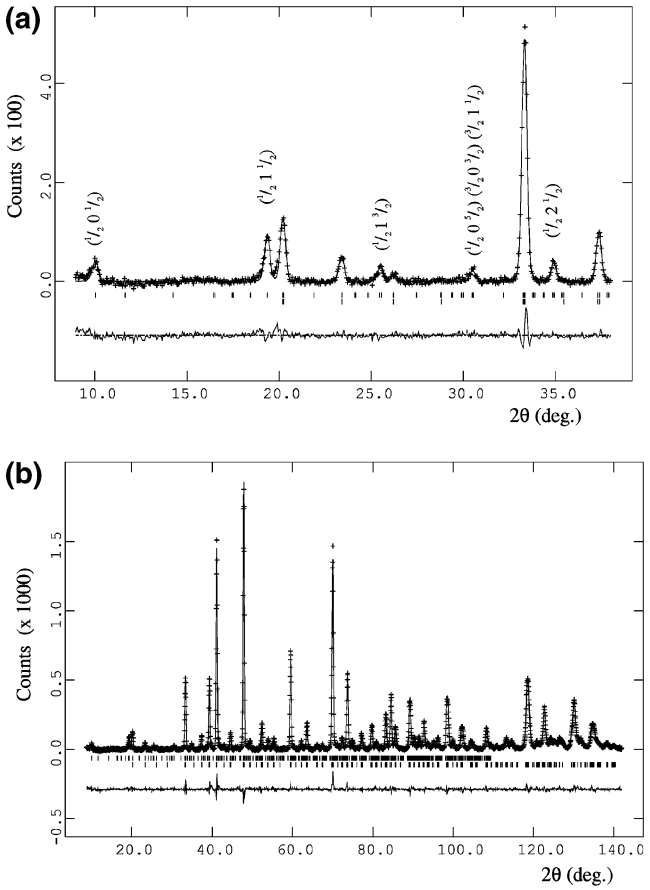

Figure 9. Observed (crosses), calculated (full line), and difference NPD Rietveld profiles for (LaSr)CoRuO$_6$ at 4 K. (a) The low angle region, with prominent magnetic superstructure reflections labeled and (b) the entire profile. Reflection markers correspond to the Bragg positions of the structural (bottom) and magnetic phase (top).

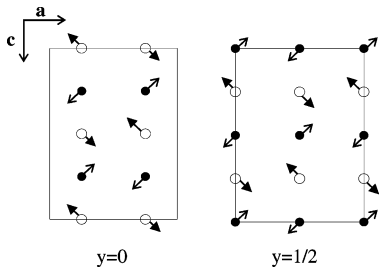

Figure 10. Spin directions in a fitted antiferromagnetic model for (LaSr)CoRuO$_6$. Co/Ru atoms are shown as open/closed circles.

components showed that the moments lie in the (010) plane and the Co moments were found to be perpendicular to the Ru moments in all refined models. One of the possible models for the magnetic structure is shown in Figure 10. This model has collinear sublattice moments with antiparallel alignment of moments related by the ($^1/_2$ $^1/_2$ $^1/_2$) translation operation. The difference in the reduced χ^2 (goodness-of-fit) between models with only Co spins [$\mu_{Co,x} = 0.85(5)\ \mu_B$, $\mu_{Co,z} = -2.05(4)\ \mu_B$, resultant $\mu_{Co} = 2.22(4)\ \mu_B$, and $\chi^2 = 2.69$] or only Ru spins [$\mu_{Ru,x} = 0.93(6)\ \mu_B$, $\mu_{Ru,z} = 2.34(4)\ \mu_B$, $\mu_{Ru} = 2.51(4)\ \mu_B$, and $\chi^2 = 2.80$] is not significant.

If the magnetic structure of (LaSr)CoRuO$_6$ is assumed to have substantial magnetic moments at both Co and Ru sites, then the possible spin arrangements such as that in Figure 10 are consistent with the presence of dominant Co−O−Ru−O−Co linear σ-superexchange interacting via vacant e_g orbitals on Ru, leading to an antiferromagnetic Co sublattice. Symmetric exchange coupling between the Co and Ru sublattices is frustrated, leaving weaker antisymmetric (Dzialoshinski−Moriya) interactions to determine the perpendicular arrangement of Co and Ru sublattice moments.

Conclusions

Powder X-ray diffraction shows the (La$_{1+x}$Sr$_{1-x}$)CoRuO$_6$ double perovskites ($-0.50 \le x \le 0.25$) to crystallize in the monoclinic $P2_1/n$ space group with a rocksalt ordered arrangement of the Co and Ru cations. The antisite disorder is small (8% inversion) for $x = 0$ and increases for $x < 0$ and $x > 0$, consistent with a decrease between the average charge and size differences of the Co and Ru states for increasing $|x|$.

Susceptibility measurements revealed ferromagnetic transitions at approximately 170 K for all compositions, but these are assigned to 0.5−2% of an SrRuO$_3$ impurity, below the limits of X-ray detection.

Variable-temperature neutron powder diffraction shows the appearance of long-range antiferromagnetic ordering ($\mathbf{k} = (^1/_2, 0, ^1/_2)$) below $T_N = 85$ K for (LaSr)CoRuO$_6$. No magnetic transition is observed at $T \approx 170$ K. The magnetic structure is indeterminate, as an infinite number of solutions varying from a purely magnetic cobalt sublattice ($\mu_{Co} = 2.2\ \mu_B$) to a purely magnetic ruthenium ($\mu_{Ru} = 2.5\ \mu_B$) sublattice or intermediate combinations with significant moments on both Ru and Co can fit the magnetic neutron intensities. Frustration of the ordering within the Co and/or Ru sublattices is evidenced.

The Neel temperatures of (La$_{1+x}$Sr$_{1-x}$)CoRuO$_6$, as determined from ZFC magnetic susceptibilities, are found to increase slightly for $x < 0$, whereas a rapid decrease for $x > 0$ is observed, signaling a strong asymmetry between hole and electron doping. Resistivity measurements showed all samples to be semiconducting 3D VRH semiconductors, where the resistivity decreases by 2 orders of magnitude for $x < 0$ but decreases much less significantly for $x > 0$.

The intrinsic properties of the (La$_{1+x}$Sr$_{1-x}$)CoRuO$_6$ solid solution as reported in this paper resemble those of the previously reported (La$_{1+x}$Ca$_{1-x}$)CoRuO$_6$ double perovskites, which also show control of the Co/Ru antisite disorder by average charge and size differences, an (indeterminate) antiferromagnetic ground state with $\mathbf{k} = (^1/_2, 0, ^1/_2)$ (below $T_N = 96$ K), and a strongly asymmetric doping dependence of the magnetization and resistivity. The discrepancies in the apparent magnetic behavior can be ascribed to the presence of a ferromagnetic SrRuO$_3$ impurity in the (La$_{1+x}$Sr$_{1-x}$)-CoRuO$_6$ samples, whereas CaRuO$_3$, if present in the (La$_{1+x}$Ca$_{1-x}$)CoRuO$_6$ samples, would be antiferromagnetic.

Acknowledgment. The authors thank the EPSRC for neutron beamtime at the ILL and Prof. T. T. M. Palstra and Ing. J. Baas for providing assistance with the transport measurements. J.W.G.B. acknowledges the EPSRC for providing a studentship.

CM0497733